Title

The cell cycle regulatory DREAM complex is disrupted by high expression of oncogenic B-Myb.

Journal

Oncogene, 38(7)

ISSN

0950-9232

Authors

Iness, Audra N
Felthousen, Jessica
Ananthapadmanabhan, Varsha
et al.

Publication Date

2019-02-01

DOI

10.1038/s41388-018-0490-y

Peer reviewed

HHS Public Access

Author manuscript

Oncogene. Author manuscript; available in PMC 2019 March 11.

Published in final edited form as:

Oncogene. 2019 February ; 38(7): 1080–1092. doi:10.1038/s41388-018-0490-y.

The cell cycle regulatory DREAM complex is disrupted by high expression of oncogenic B-Myb

Audra N. Iness[1], **Jessica Felthousen**[1], **Varsha Ananthapadmanabhan**[1], **Fatmata Sesay**[1], **Siddharth Saini**[1], **Keelan Z. Guiley**[2], **Seth M. Rubin**[2], **Mikhail Dozmorov**[3], and **Larisa Litovchick**[1,*]

[1]Division of Hematology, Oncology and Palliative Care and Massey Cancer Center, Virginia Commonwealth University, Richmond, VA 23298, USA

[2]Department of Chemistry and Biochemistry, University of California, Santa Cruz, CA 95064, USA

[3]Department of Biostatistics, Virginia Commonwealth University, Richmond, VA, 23298, USA

Abstract

Overexpression of the oncogene *MYBL2* (B-Myb) is associated with increased cell proliferation and serves as marker of poor prognosis in cancer. However, the mechanism by which B-Myb alters the cell cycle is not fully understood. In proliferating cells, B-Myb interacts with the MuvB core complex including LIN9, LIN37, LIN52, RBBP4, and LIN54, forming the MMB (Myb-MuvB) complex, and promotes transcription of genes required for mitosis. Alternatively, the MuvB core interacts with Rb-like protein p130 and E2F4-DP1 to form the DREAM complex that mediates global repression of cell cycle genes in G0/G1, including a subset of MMB target genes. Here, we show that overexpression of B-Myb disrupts the DREAM complex in human cells, and this activity depends on the intact MuvB-binding domain in B-Myb. Furthermore, we found that B-Myb regulates the protein expression levels of the MuvB core subunit LIN52, a key adaptor for assembly of both the DREAM and MMB complexes, by a mechanism that requires S28 phosphorylation site in LIN52. Given that high expression of B-Myb correlates with global loss of repression of DREAM target genes in breast and ovarian cancer, our findings offer mechanistic insights for aggressiveness of cancers with *MYBL2* amplification, and establish the rationale for targeting B-Myb to restore cell cycle control.

Keywords

DYRK1A; harmine; transcription; cell cycle; protein complex; protein degradation

*Correspondence: larisa.litovchick@vcuhealth.org.

Conflicts of Interest

The authors have no conflicts of interest to disclose.

Introduction

Since its discovery in 1988, several studies have established *MYBL2* (encoding B-Myb) as a clinically important oncogene [25, 41]. Indeed, *MYBL2* is part of the Onco*type* DX® screening panel and validated DCIS (Ductal Carcinoma *in situ*) Score™, used to predict the risk of local recurrence in patients with breast cancer [1, 36]. However, the specific cellular mechanisms of B-Myb's oncogenic activities are not fully understood.

Previous studies characterized B-Myb as a transcription factor involved in cell cycle regulation and expressed in proliferating cells [24]. The essential role of B-Myb for cell proliferation is evidenced by failure of inner cell mass formation and embryonic death of *MYBL2* knock-out mice [39]. Oncogenic functions of B-Myb have been attributed to its transcriptional activity, resulting in deregulated cell cycle gene expression [12, 23, 33]. Studies in *Drosophila* and human cells revealed that B-Myb regulates transcription of developmental and cell cycle genes as part of an evolutionarily conserved multi-subunit protein complex, which shares common subunits with DNA-binding complexes formed by retinoblastoma (RB) family members [7, 30]. In *Drosophila*, Myb functions as part of the dREAM (RB, E2F, and Myb) complex that includes five proteins homologous to the products of the *C. elegans* multi-vulva class B (MuvB) genes: LIN9, LIN37, LIN52, LIN53/RBBP4 and LIN54 [16, 17]. In the mammalian cell cycle, the orthologous DREAM (DP, RB-like, E2F, and MuvB) complex does not include Myb, and promotes cell cycle exit by repressing more than 800 cell cycle genes (including *MYBL2*) in quiescent cells (Fig. 1A) [18, 27, 34]. Interestingly, although pRb does not interact with the MuvB core, which only accommodates RB-like p130 or p107 [9, 18], this tumor suppressor functionally cooperates with DREAM in establishing and maintaining quiescence [22]. DREAM is assembled in G0/G1 and depends on DYRK1A (dual-specificity tyrosine-phosphorylation regulated kinase 1A) phosphorylation of LIN52 (MuvB subunit) at serine 28 (S28) for bringing together p130 and the MuvB core[19]. Upon cell cycle progression, p130 is phosphorylated by cyclin-dependent kinases (CDKs) and dissociates from MuvB [9]. In the S phase, MuvB binds B-Myb, forming the MMB (Myb-MuvB) complex that cooperates with FOXM1 transcription factor to activate G2/M gene expression [4, 29]. Importantly, LIN52 is required for MuvB to bind B-Myb, making LIN52 an essential component of both the DREAM and MMB complexes [9]. Unlike DREAM, LIN52 binding to B-Myb is independent of S28 phosphorylation. Interestingly, the *Drosophila* dREAM complex includes the Myb and RB proteins together with MuvB, whereas the mammalian DREAM and MMB complexes exist in a cell cycle-dependent, mutually exclusive manner [15, 17, 18, 27]. An *in vitro* study with reconstituted human complexes demonstrated that both B-Myb and p130 could simultaneously bind to MuvB, suggesting that their mutually exclusive binding *in vivo* is not due to structural constraints [9].

Studies of DREAM disruption by genome editing show that DREAM-deficient cells have abnormal binding of B-Myb to MuvB and loss of DREAM target gene repression under the conditions of G0/G1 cell cycle arrest [8, 22]. Since B-Myb overexpression also deregulates the cell cycle [31, 32], we investigated whether B-Myb, when over-expressed, could play a causal role in disrupting DREAM. Our data shown here support the regulation of DREAM by B-Myb as a potential mechanism for the cell cycle defects observed in cancers with high B-Myb levels. Furthermore, we demonstrate that increased expression of B-Myb disrupts

DREAM by compromising recruitment of LIN52 to the complex, and describe the regulation of LIN52 expression by B-Myb. These findings implicate global cell cycle deregulation by disrupting the DREAM repressor function as a means by which B-Myb exerts its oncogenic effects and promotes cancer progression.

Results

B-Myb inhibits DREAM assembly in non-transformed human fibroblasts

B-Myb overexpression is associated with a proliferative phenotype, which could be due to loss of DREAM function. Therefore, we assessed the effect of B-Myb gain of function on DREAM formation by expressing HA-B-Myb in non-transformed human fibroblasts immortalized with hTERT (BJ-hTERT) [11, 19]. We first measured the proliferation rate of cells expressing HA-B-Myb compared to control cells expressing HA-GFP, using an ATP-dependent metabolic assay [21]. As expected, BJ-hTERT cells expressing HA-B-Myb exhibited a significantly greater proliferation rate than controls (Fig. 1B). We then determined the effect of high B-Myb levels on DREAM assembly. While both the LIN37-p130 complexes (specific to DREAM) and LIN37-B-Myb complexes (corresponding to MMB) were present in the asynchronously cycling control cells, B-Myb overexpression resulted in almost no detectable p130 co-precipitating with LIN37. To clarify the effect of B-Myb on DREAM, we serum starved these cells to induce DREAM formation. As expected, DREAM formation increased in serum-starved control BJ-hTERT cells. Although B-Myb overexpressing cells formed p130/LIN37 complexes, DREAM levels were significantly diminished with HA-B-Myb expression (Fig. 1C, D). This result suggests that even in the presence of high B-Myb, DREAM disassembly remains partially dependent on environmental factors. Similar findings were obtained under alternative growth arrest conditions with palbociclib (CDK4/6 inhibitor) treatment (Fig. S1A, B). Therefore, although we previously showed that p130 and B-Myb could simultaneously bind to MuvB [9], here we observed that overexpression of B-Myb in non-transformed cells results in MMB formation under conditions that normally favor DREAM assembly.

B-Myb requires binding to MuvB for DREAM disassembly

B-Myb overexpression did not affect the interaction between LIN37 and MuvB proteins LIN9 and LIN52. However, we noted an increased abundance of LIN9 and LIN52 proteins in the non-starved B-Myb overexpressing BJ-hTERT cells compared to control (Fig. 1C, E). This could be attributable to transcriptional regulation, as DREAM binds to *LIN9* and *LIN52* promoters [6]. In line with DREAM-mediated repression, RT-qPCR analysis confirmed downregulation of LIN9 and LIN52 mRNA with serum starvation. In non-starved cells, HA-B-Myb was significantly associated with increased *LIN9* and *LIN52* expression, a trend also observed with both genes in the serum starved state (Fig. S1C, D). Given a modest 1.5-fold increase of *LIN52* mRNA levels in the presence of HA-B-Myb, we measured LIN52 protein stability in BJ-hTERT cells using cycloheximide (CHX) chase assays and found that it was more abundant after 10h of CHX treatment in the HA-B-Myb-expressing cells as compared with control (Fig. S1F). Since LIN52 is a MuvB component essential for formation of both DREAM and MMB, we further investigated the effect of B-Myb overexpression on LIN52.

In addition to increased expression, we noted alterations in the relative abundance of S28-phosophorylated and un-phosphorylated LIN52 in the presence of HA-B-Myb (Fig. 1C, E). We have previously shown that slower migrating form of LIN52 appears when this protein is phosphorylated at S28 by DYRK1A kinase [19]. Using a phospho-specific antibody, we confirmed that relative abundance of S28-phosphorylated LIN52 was decreased in the presence of HA-B-Myb and not associated with changes in DYRK1A level or kinase activity (Fig. 1E, S1E), suggesting that B-Myb could inhibit DREAM assembly by interfering with the key phosphorylation event required for MuvB binding to p130 [6]. To test the importance of MuvB binding for B-Myb-mediated DREAM disruption and regulation of LIN52, we compared BJ-hTERT cell lines expressing either wild-type HA-B-Myb or a MuvB-binding deficient (MBD) mutant Q674A/M677A-B-Myb [10]. As shown in Fig. 1F, DREAM assembly and LIN52 protein expression were unaffected by the presence of MBD HA-B-Myb, suggesting that MuvB binding is essential for these effects.

To further validate and characterize the effect of B-Myb on DREAM assembly, we used T98G glioblastoma cells because they have been studied extensively in cell cycle research, including initial characterization of DREAM and MMB [18]. Although this cancer cell line lacks *MYBL2* amplification, T98G cells express readily detectable levels of B-Myb (unlike BJ-hTERT), making them amenable to both loss and gain of function studies of B-Myb [18, 19, 31, 38]. Similar to BJ-hTERT cells (Fig. 1C, F), expression of wild-type B-Myb, but not the MBD mutant resulted in decreased DREAM assembly (Fig. 2A). Consistent with this result, we observed that the endogenous LIN52 protein was more abundant and relatively less phosphorylated in the presence of HA-B-Myb than in parental T98G cells, or the cells expressing MBD HA-B-Myb (Fig. 2B). These findings reinforced the important role of B-Myb-MuvB binding not only for DREAM disruption, but also for influencing LIN52 protein, and led us to further investigate regulation of LIN52 as a novel mechanism by which B-Myb impacts cell cycle gene expression.

LIN52 expression is controlled at the protein level

Since B-Myb disrupts DREAM and also increases LIN52 protein abundance, we tested whether DREAM assembly is influenced by ectopic overexpression of LIN52 alone. However, analysis of T98G cells stably expressing LIN52-V5, HA-B-Myb, or both, showed no substantial impact of ectopically expressed LIN52 on DREAM assembly (Fig. 2C). Furthermore, LIN52-V5 appeared to replace endogenous LIN52 from LIN37 complexes, likely because of decreased endogenous LIN52 expression in the presence of LIN52-V5 (Fig. 2D). RT-qPCR analysis with primers specific for endogenous LIN52 mRNA revealed no significant changes in the presence of LIN52-V5, indicating that LIN52 downregulation occurs at the protein level (Fig. 2E). In support of LIN52 regulation at the protein level, expression of GFP-LIN52 fusion protein was markedly reduced, compared with the GFP-only control, despite similar expression of control dsRed protein produced from the same mRNA transcript using Global Protein Stability (GPS) expression vectors (Fig. S2) [44]. This prompted us to assess the stability of both endogenous and ectopically expressed LIN52 using CHX chase assays. We noted that both endogenous and ectopically expressed LIN52 proteins were both markedly depleted after 3h of CHX treatment (Fig. 2F), suggesting that LIN52 was less stable in T98G cells than in BJ-hTERT (Fig. S1F). We were not able to

estimate the turnover rate of endogenous LIN52 in LIN52-V5-expressing cells because of its low expression. Of note, we did not observe significant degradation of MuvB protein LIN37 under these conditions.

To further validate our finding that B-Myb regulates LIN52 protein expression, we altered B-Myb levels in T98G cells stably expressing LIN52-V5. As in case of endogenous LIN52, overexpression of B-Myb resulted in increased expression of the LIN52-V5 protein in T98G cells (Fig. 2G). Furthermore, siRNA knockdown of B-Myb led to downregulation of LIN52-V5 as well as the endogenous LIN52 protein (Fig. 2H). To determine the biological relevance of our findings, we monitored changes in LIN52 abundance and phosphorylation, in the context of the MuvB core, during cell cycle progression. T98G cells were synchronized in G0/G1 by serum deprivation, then released into the cell cycle by serum re-stimulation, and collected at different time points for LIN37 IP. As shown in Fig. 2I, appearance of the faster migrating (un-phosphorylated) form of LIN52 increased co-incidentally with loss of p130 and accumulation of B-Myb in the LIN37 immunoprecipitates, consistent with B-Myb's effect on LIN52 phosphorylation. Together, our data presented above show that B-Myb is able to disrupt DREAM assembly when highly expressed, and support the role of B-Myb in regulation of LIN52 expression at the protein level.

Regulation of LIN52 stability by B-Myb requires intact S28 residue

We then examined the relative effects of B-Myb expression and S28 phosphorylation on LIN52 protein stability in a series of quantitative CHX assays by comparing the effect of B-Myb on wild-type LIN52 and non-phosphorylatable S28A-LIN52 mutant using established T98G cell lines [19]. The S28A mutation abolishes the DYRK1A-phosphorylation site essential for DREAM formation without interfering with the MMB complex assembly [9]. Using CHX assays, we determined that the half-life of wild type LIN52-V5 in T98G cells was approximately 3h (Fig. 3A, B). Using MG132 together with CHX blocked the degradation of LIN52-V5 in this assay, suggesting that LIN52 degradation involves the proteasome. As expected, expression of HA-B-Myb in these cells resulted in significant stabilization of ectopically expressed LIN52-V5 by approximately 40% (Fig. 3A, C). Interestingly, the LIN52-S28A mutant remained significantly more abundant at the 3h time point than wild-type LIN52-V5 (Fig. 3B). Furthermore, whereas the stability of wild-type LIN52-V5 was significantly impacted by the presence of HA-B-Myb, stability of the S28A mutant LIN52 remained unchanged (Fig. 3A, C). Despite this finding, we noted that there is an apparent persistence of the upper LIN52 band over the time course of CHX treatment, suggesting that a subset of phosphorylated LIN52 may be protected from degradation. We also monitored levels of LIN9, LIN37 and p130 in the same CHX chase experiments, and stability of these proteins did not show the same dependency on B-Myb as LIN52 (Fig. 3A). Together, these data show that stability of LIN52 is regulated by B-Myb and requires an intact S28 residue.

These conclusions were additionally supported when LIN52 stability was analyzed under the conditions of B-Myb knock-down. Indeed, LIN52-V5 protein decayed more rapidly after CHX treatment in T98G cells with RNAi-mediated B-Myb knock-down compared to cells

transfected with non-targeting (NT) control siRNA (Fig. 4A, B). Here, we again found that B-Myb exhibits no significant effect on LIN52-S28A-V5 protein stability. Since B-Myb is still able to bind to LIN52-S28A-V5 [19], these results suggest that phosphorylation at the S28 plays a role in regulating LIN52 levels.

DYRK1A regulates LIN52 stability

Given that LIN52 phosphorylation at S28 is mediated by DYRK1A [19], we wanted to determine the role of DYRK1A in regulating LIN52 levels. We used the CRISPR/Cas9 genome editing approach [28] to generate T98G cells devoid of DYRK1A protein (DYRK1A-KO) (Fig. S3). To validate the specificity of DYRK1A as S28-LIN52 kinase, we performed an *in vitro* kinase assay with extracts from T98G parental and DYRK1A KO cells using WB detection of pS28-LIN52 as readout. As shown in Fig. 5A, S28-LIN52 kinase activity was greatly diminished in T98G DYRK1A KO cells compared to control. LIN52 was expressed at higher steady-state levels and appeared in a predominantly un-phosphorylated form in DYRK1A-KO cells or in T98G cells treated with a DYRK1A kinase inhibitor, harmine [3] (Fig. 5B). Phosphospecific WB confirmed a substantial reduction in S28-phosphorylated LIN52 with either harmine treatment or DYRK1A KO. The remaining pS28-LIN52 in DYRK1A-inhibited cells could be due to phosphorylation by alternative LIN52 kinases, such as CDKs [14]. Additionally, DYRK1B, a homologue of DYRK1A that is less abundant in T98G cells, could partly compensate for the lack of DYRK1A in KO cells [19].

We then performed CHX chase experiments and showed that the stability of endogenous LIN52 is enhanced when DYRK1A is absent or inhibited by harmine (Fig. 5C, D). RT-qPCR analysis revealed a modest increase in LIN52 mRNA expression when DYRK1A is knocked out or inhibited (Fig. 5E), suggesting that LIN52 is also regulated by DYRK1A at the level of transcription. Taken together, our data demonstrate that LIN52 is regulated at the protein level, and that DYRK1A-dependent phosphorylation is involved in the control of LIN52 stability.

Model of B-Myb-mediated DREAM disruption in cancer

Finally, we sought to apply our model of B-Myb-mediated DREAM disruption to clinically relevant cancer models, such as SKOV3 serous ovarian carcinoma cells known to harbor *MYBL2* gene amplification [2]. As shown in Fig. 6A, B-Myb knock-down resulted in downregulation of LIN52, as we observed previously in T98G cells expressing LIN52-V5 (Fig. 2H). Asynchronously growing SKOV3 cells contain low steady state levels of DREAM, and a robust increase of DREAM formation was detected after RNAi-mediated knock-down of B-Myb (Fig. 6B and6C). RT-qPCR analysis shown in Figure 6D confirms the knockdown of *MYBL2*, as well as a decreased expression of a known MMB-target gene *CCNB2* [6]. Importantly, this analysis also revealed decreased expression of a representative DREAM-only target gene (*FOXM1*), in agreement with the observed increase of the DREAM formation (Fig. 6C). LIN52 mRNA levels were not significantly influenced by depletion of B-Myb, further supporting the conclusion that B-Myb regulates LIN52 predominantly at the protein level.

To further investigate the functional relationship between B-Myb level and regulation of cell cycle dependent transcription, we analyzed gene expression data from The Cancer Genome Atlas (TCGA). We first looked at the *MYBL2* gene expression across all cancers and the corresponding normal tissue samples, when available. As previously reported, the *MYBL2* gene was overexpressed in multiple cancer types (Fig. S4A). For further analysis of transcriptome changes associated with high *MYBL2* expression, we chose to focus on high grade serous ovarian carcinoma (HGSOC), since *MYBL2* gene copy number gain is present in 55% of the TCGA HGSOC samples and associated with a poor prognosis (data not shown) [40]. Similar analyses were conducted in parallel for breast cancer, for which the significance of B-Myb overexpression is well-documented [5, 13, 37, 41]. We first validated that *MYBL2* genomic amplification correlated with increased B-Myb mRNA expression (Fig. S4B, C) as well as with significant up-regulation of cell cycle regulated genes (Table S1, S2) then proceeded to characterize the most differentially expressed genes between tumor samples with high and low *MYBL2* expression levels. As expected, we found that most differentially expressed genes in both cancer types were highly enriched in functional gene ontology categories representing cell cycle processes. Furthermore, both MMB and DREAM target genes were overrepresented among the most differentially expressed genes in the high-*MYBL2* samples (Fig. S4C, D), and high B-Myb levels were associated with increased MMB and DREAM target gene expression. Remarkably, the top 50 upregulated genes associated with high *MYBL2* in breast cancer analysis, and top 49 genes in HGSOC, have been previously annotated as DREAM target genes identified in global location studies [6, 18]. Since MMB does not regulate some of these genes directly, this finding supports the model whereby B-Myb-mediated DREAM disruption plays a role in deregulation of cell cycle gene expression program in cancers with high B-Myb expression (Fig. 6E, F). Overall, our data support a model by which B-Myb accumulation during cell cycle progression or due to overexpression in cancer interferes with LIN52 phosphorylation at S28 by DYRK1A kinase that is required for the DREAM assembly. This leads to increased LIN52 abundance and stability, while also disrupting DREAM assembly, so that more MMB complex is formed, ultimately resulting in compromised repression of DREAM-target genes (Fig. 7).

Discussion

The DREAM and MMB complexes share the common MuvB core and appear to assemble in a mutually exclusive manner during mammalian cell cycle progression [7, 30]. Several studies demonstrated that the DREAM and MMB complexes exist during different stages of the cell cycle with minimal overlap during the G1-S transition [18, 19, 27, 29]. It was also shown that release of the MuvB core from DREAM requires cyclin-CDK phosphorylation of DREAM components and that chemical inhibition of either CDK4 or CDK2 stabilizes the DREAM under the conditions of cell cycle re-entry [9, 26]. However, since B-Myb was not expressed in CDK-inhibited cells, it was unclear whether B-Myb could play an active role in DREAM disassembly. Here we show that DREAM is disrupted in human cells when B-Myb is highly expressed and is able to bind to MuvB core. Given our previous observation and studies in *Drosophila* that both RB-like protein and B-Myb can simultaneously associate with MuvB, we do not propose that p130 and B-Myb compete for LIN52 binding [9, 15]. Alternatively, we suggest that B-Myb promotes DREAM disassembly by inhibiting LIN52

phosphorylation. LIN52 is then stabilized for formation of additional MMB complexes that, in turn, are required to facilitate transcription of the duplicated genome after DNA replication is complete in late S-G2 phases. In this model, CDKs and B-Myb could cooperate to establish a positive feedback loop to disrupt the DREAM and relieve the E2F-mediated repression of cell cycle genes.

We found that levels of LIN52 and LIN9 in the cell are tightly controlled and regulated by B-Myb, both directly by transcription of mRNA and, in case of LIN52, also at the post-transcriptional level. Regulation of LIN52 by B-Myb is especially interesting given its role as the key MuvB component required for assembly of both DREAM and MMB. We observe that LIN52 is tightly regulated at the protein level and ectopic LIN52 expression results in increased turnover of the protein by both proteasome-dependent and independent mechanisms. We have previously demonstrated that the phosphorylated S28 residue plays a key role in direct binding of LIN52 to p130, required for DREAM assembly [9, 19]. Our observation that overexpression of B-Myb in human cells promotes accumulation of un-phosphorylated LIN52 could partly explain the increased stability of LIN52 protein in the presence of highly expressed B-Myb. In support of this mechanism, unlike the wild-type LIN52, changes in B-Myb level do not impact the stability of LIN52-S28A. It remains to be established how B-Myb can interfere with LIN52 phosphorylation and degradation. B-Myb could stabilize LIN52 by regulating expression of proteins that degrade or stabilize LIN52, or by recruiting a phosphatase that will remove the LIN52 phospho-S28 mark. It is also possible that steric hindrance by B-Myb could block DYRK1A's access to the S28 site in LIN52. In our study, inhibition of S28A LIN52 phosphorylation consistently resulted in accumulation of total LIN52 protein. However, given the continued presence of the slower migrating form of LIN52 in CHX chase assays, phosphorylation state does not completely account for LIN52 protein regulation. Therefore, further studies are needed to investigate these mechanisms.

This study also provides important insights into subunit interactions within the MuvB complex. Here, LIN52 appears to have shorter half-life than LIN9 or LIN37, possibly because of its special regulatory role. Indeed, LIN52 is required for both DREAM and MMB formation and makes direct contact with both p130/p107 and B-Myb ([9] and [10]). Therefore, changes in LIN52 levels will influence the overall functional integrity of MuvB core. This is supported by diminished co-immunoprecipitation of MuvB complex components when LIN52 is depleted by shRNA [19]. However, other studies have shown that LIN37 and LIN54 are also downregulated when LIN9 is depleted, suggesting a possibility that some of MuvB subunits need to co-fold together during translation [34]. This is supported by our observation that expression of LIN52-GFP fusion protein was not rescued to the GFP-control level by inhibition of proteasome. It will be interesting to determine whether this phosphorylation-independent mechanism controlling LIN52 stability could involve cellular chaperone complexes, such as CCR4-NOT, that mediate degradation of misfolded proteins [43]. A recent study found that in the LIN37 knockout cells, the remaining MuvB subunits were normally expressed and formed a complex capable of binding to either p130, or B-Myb, and while the MMB function remained intact, the DREAM repressor function was compromised [22]. Together, these findings suggest that the abundance of MuvB core could be important for its biological functions, for example to ensure the specificity of binding to the promoter sites,

and needs to be tightly regulated. In the future, it will be interesting to investigate the consequences of failure to maintain the proper levels of MuvB core subunits in the cell.

B-Myb is overexpressed in many types of cancer and is recognized as a poor prognostic factor, but the known role of B-Myb as a transcription factor required for mitotic progression does not fully explain its established association with a more aggressive cancer phenotype. Our finding that B-Myb disrupts the DREAM complex in cells could explain why high expression of B-Myb leads to de-repression of DREAM cell cycle gene targets in human cancers (Fig. 6D, E). B-Myb expression in cancers could be upregulated due to a *MYBL2* gene copy number gain or amplification [41]. Since *MYBL2* itself is a DREAM target gene, this might create a positive feedback loop in which increased B-Myb expression perpetuates DREAM disruption and further loss of transcriptional regulation. Several of the MMB downstream targets upregulated in late S-G2 phases of the cell cycle, such as Aurora kinase A, Polo-like kinase 1 and others have been proposed for developing anti-cancer therapies [12]. Better understanding of the mechanisms that bring about high expression of these genes in cancer will be important to inform the future pre-clinical and clinical studies and to optimize patient stratification. Overall, we have shown a novel model describing some of the molecular processes underlying deregulated cell cycle gene expression in cancers with B-Myb amplification or overexpression. These findings argue that B-Myb is not only a negative prognostic factor through increased MMB formation and activation of the mitotic gene expression program, but also through decreased DREAM assembly and loss of repression of more than 800 cell cycle-regulated genes. Further studies with tumor samples are needed to validate our model in patients and evaluate methods of targeting B-Myb to restore cell cycle control.

Materials and Methods

Cells

T98G and SKOV3 cell lines were purchased from ATCC and used at low passage (<10) with routine mycoplasma testing. T98G cells stably expressing V5-tagged LIN52 or LIN52-S28A and BJ-hTERT cells were previously described [18, 19]. T98G and BJ-hTERT cells were infected with a HA-FLAG-B-Myb (WT) or MuvB-binding deficient mutant B-Myb (Q674A/M677A) retroviruses produced using pMSCV-Puro vector, and selected on 1 μg/ml puromycin [18, 19]. T98G DYRK1A KO cells were established using GeneArt CRISPR nuclease vector with OFP reporter (Life Technologies) harboring a DYRK1A-specific guiding RNA sequence (Supplemental data and Table S3). For cell proliferation assay, 3,000 cells were plated per well of a 96-well plate, and luminescence was measured using ATPLite kit (PerkinElmer) at days 3 and 5. Invitrogen RNAiMAX™ was used for transfections of Ambion® Silencer® Select MYBL2 (s9117 and s9118), DYRK1A (s4399) and Negative Control No. 1 (4390843) siRNA oligonucleotides. Transfections of plasmid DNA were performed using polyethylenimine [20].

Immunoprecipitations and Western blots

Antibodies for MuvB complex components LIN9, LIN37, LIN52 and pS28-LIN52 were previously described [18, 19]. Commercially available antibodies are listed in Table S4. For

IP/WB assays using rabbit antibodies, Reliablot® Western blot kit (Bethyl Inc.) was used for detection. Protein band densities were quantified using ImageJ software and statistically analyzed by Student's two-tailed t-test to compare means of 3 biological repeats [35].

Quantitative PCR

RNA was isolated using TRIzol reagent (Invitrogen) and used to synthesize cDNA using SensiFAST™ kit (Bioline). qPCR with Maxima SYBR Green/ROX master mix (ThermoFisher) and gene specific primers (Table S5) was performed using Applied Biosystems 7900HT. Fold changes in mRNA expression relative to controls were calculated using the 2ΔΔCt methodology.

In vitro kinase assay

Cell extracts from control and DYRK1A-KO T98G cells, or BJ-hTERT cell lines (3 mg/ml) were prepared using EDTA-free EBC buffer [18, 19] supplemented with phosphatase inhibitors, 2 mM DTT, 10 mM MgCl2, 10 mM MnCl2 and 200 μM ATP, and incubated at 30°C with 6 ng/μl GST-LIN52 in a 100 μl reaction volume. Reactions were terminated by adding SDS-PAGE loading buffer and heating at 95°C for 10 min, and analyzed by WB.

Biostatistics

To calculate statistical significance, data from at least 3 biological replicates was analyzed using two-tailed Student's t-test. For TCGA data analysis, open access gene copy number and expression data was obtained as described in Supplemental data section. For differential expression analysis, samples in the selected cancer cohort were sorted by expression of *MYBL2*. Differentially expressed genes were detected between samples in the upper 75 and lower 25 percentiles of the expression gradient using the limma R package v. 3.32.6. P-values were corrected for multiple testing using False Discovery Rate (FDR) method. Genes differentially expressed at FDR < 0.01 were selected for Metascape (http://metascape.org/) functional enrichment analysis using the latest 03–16-2017 database version [42]. Top 50 genes up- and downregulated in the selected cancer were also overlapped with DREAM and MMB targets [6, 18, 29].

Supplementary Material

Refer to Web version on PubMed Central for supplementary material.

Acknowledgements

We thank James DeCaprio and Iain Morgan for critical reading the manuscript, and Sophia Gruszecki for technical support. This project was supported in part by R01CA188571 (L.L.), R01CA132685 and R01GM124148 (S.M.R.), and F30CA221004 (A.N.I.).

References

1. Allegra CJ, Aberle DR, Ganschow P, Hahn SM, Lee CN, Millon-Underwood S et al. National Institutes of Health State-of-the-Science Conference statement: Diagnosis and Management of Ductal Carcinoma In Situ September 22–24, 2009. Journal of the National Cancer Institute 2010; 102: 161–169. [PubMed: 20071686]

2. Barretina J, Caponigro G, Stransky N, Venkatesan K, Margolin AA, Kim S et al. The Cancer Cell Line Encyclopedia enables predictive modelling of anticancer drug sensitivity. Nature 2012; 483: 603–607. [PubMed: 22460905]

3. Becker W, Sippl W. Activation, regulation, and inhibition of DYRK1A. The FEBS journal 2011; 278: 246–256.

4. Chen X, Muller GA, Quaas M, Fischer M, Han N, Stutchbury B et al. The forkhead transcription factor FOXM1 controls cell cycle-dependent gene expression through an atypical chromatin binding mechanism. Mol Cell Biol 2012; 33: 227–236. [PubMed: 23109430]

5. Dedic Plavetic N, Jakic-Razumovic J, Kulic A, Vrbanec D. Prognostic value of proliferation markers expression in breast cancer. Medical oncology 2013; 30: 523. [PubMed: 23468220]

6. Fischer M, Grossmann P, Padi M, DeCaprio JA. Integration of TP53, DREAM, MMB-FOXM1 and RB-E2F target gene analyses identifies cell cycle gene regulatory networks. Nucleic acids research 2016; 44: 6070–6086. [PubMed: 27280975]

7. Fischer M, Muller GA. Cell cycle transcription control: DREAM/MuvB and RB-E2F complexes. Crit Rev Biochem Mol Biol 2017: 1–25.

8. Forristal C, Henley SA, MacDonald JI, Bush JR, Ort C, Passos DT et al. Loss of the mammalian DREAM complex deregulates chondrocyte proliferation. Molecular and cellular biology 2014; 34: 2221–2234. [PubMed: 24710275]

9. Guiley KZ, Liban TJ, Felthousen JG, Ramanan P, Litovchick L, Rubin SM. Structural mechanisms of DREAM complex assembly and regulation. Genes & development 2015; 29: 961–974. [PubMed: 25917549]

10. Guiley KZ, Iness AN, Saini S, Tripathi S, Lipsick JS, Litovchick L, Rubin SM. Structural mechanism of Myb-MuvB assembly. Proc Natl Acad Sci U S A. 2018 9 17 [Epub ahead of print] PubMed PMID: 30224471.

11. Hahn WC, Counter CM, Lundberg AS, Beijersbergen RL, Brooks MW, Weinberg RA. Creation of human tumour cells with defined genetic elements. Nature 1999; 400: 464–468. [PubMed: 10440377]

12. Iltzsche F, Simon K, Stopp S, Pattschull G, Francke S, Wolter P et al. An important role for Myb-MuvB and its target gene KIF23 in a mouse model of lung adenocarcinoma. Oncogene 2017; 36: 110–121. [PubMed: 27212033]

13. Inoue K, Fry EA. Novel Molecular Markers for Breast Cancer. Biomarkers in cancer 2016; 8: 25–42. [PubMed: 26997872]

14. Iwahori S, Kalejta RF. Phosphorylation of transcriptional regulators in the retinoblastoma protein pathway by UL97, the viral cyclin-dependent kinase encoded by human cytomegalovirus. Virology 2017; 512: 95–103. [PubMed: 28946006]

15. Korenjak M, Taylor-Harding B, Binne UK, Satterlee JS, Stevaux O, Aasland R et al. Native E2F/RBF complexes contain Myb-interacting proteins and repress transcription of developmentally controlled E2F target genes. Cell 2004; 119: 181–193. [PubMed: 15479636]

16. Korenjak M, Brehm A. E2F-Rb complexes regulating transcription of genes important for differentiation and development. Curr Opin Genet Dev 2005; 15: 520–527. [PubMed: 16081278]

17. Lewis PW, Beall EL, Fleischer TC, Georlette D, Link AJ, Botchan MR. Identification of a Drosophila Myb-E2F2/RBF transcriptional repressor complex. Genes & development 2004; 18: 2929–2940. [PubMed: 15545624]

18. Litovchick L, Sadasivam S, Florens L, Zhu X, Swanson SK, Velmurugan S et al. Evolutionarily conserved multisubunit RBL2/p130 and E2F4 protein complex represses human cell cycle-dependent genes in quiescence. Mol Cell 2007; 26: 539–551. [PubMed: 17531812]

19. Litovchick L, Florens L, Swanson SK, Washburn MP, DeCaprio JA. DYRK1A protein kinase promotes quiescence and senescence through DREAM complex assembly. Genes Dev 2011; 25: 801–813. [PubMed: 21498570]

20. Longo PA, Kavran JM, Kim MS, Leahy DJ. Transient mammalian cell transfection with polyethylenimine (PEI). Methods in enzymology 2013; 529: 227–240. [PubMed: 24011049]

21. Lundin A, Hasenson M, Persson J, Pousette A. Estimation of biomass in growing cell lines by adenosine triphosphate assay. Methods in enzymology 1986; 133: 27–42. [PubMed: 3821540]

22. Mages CF, Wintsche A, Bernhart SH, Muller GA. The DREAM complex through its subunit Lin37 cooperates with Rb to initiate quiescence. Elife 2017; 6.
23. Musa J, Aynaud MM, Mirabeau O, Delattre O, Grunewald TG. MYBL2 (B-Myb): a central regulator of cell proliferation, cell survival and differentiation involved in tumorigenesis. Cell death & disease 2017; 8: e2895. [PubMed: 28640249]
24. Ness SA. Myb protein specificity: evidence of a context-specific transcription factor code. Blood cells, molecules & diseases 2003; 31: 192–200.
25. Nomura N, Takahashi M, Matsui M, Ishii S, Date T, Sasamoto S et al. Isolation of human cDNA clones of myb-related genes, A-myb and B-myb. Nucleic acids research 1988; 16: 11075–11089. [PubMed: 3060855]
26. Odajima J, Saini S, Jung P, Ndassa-Colday Y, Ficaro S, Geng Y et al. Proteomic Landscape of Tissue-Specific Cyclin E Functions in Vivo. PLoS genetics 2016; 12: e1006429. [PubMed: 27828963]
27. Pilkinton M, Sandoval R, Colamonici OR. Mammalian Mip/LIN-9 interacts with either the p107, p130/E2F4 repressor complex or B-Myb in a cell cycle-phase-dependent context distinct from the Drosophila dREAM complex. Oncogene 2007; 26: 7535–7543. [PubMed: 17563750]
28. Ran FA, Hsu PD, Wright J, Agarwala V, Scott DA, Zhang F. Genome engineering using the CRISPR-Cas9 system. Nature protocols 2013; 8: 2281–2308. [PubMed: 24157548]
29. Sadasivam S, Duan S, DeCaprio JA. The MuvB complex sequentially recruits B-Myb and FoxM1 to promote mitotic gene expression. Genes & development 2012; 26: 474–489. [PubMed: 22391450]
30. Sadasivam S, DeCaprio JA. The DREAM complex: master coordinator of cell cycle-dependent gene expression. Nature reviews Cancer 2013; 13: 585–595. [PubMed: 23842645]
31. Sala A, Casella I, Bellon T, Calabretta B, Watson RJ, Peschle C. B-myb promotes S phase and is a downstream target of the negative regulator p107 in human cells. The Journal of biological chemistry 1996; 271: 9363–9367. [PubMed: 8621601]
32. Sala A, Kundu M, Casella I, Engelhard A, Calabretta B, Grasso L et al. Activation of human B-MYB by cyclins. Proceedings of the National Academy of Sciences of the United States of America 1997; 94: 532–536. [PubMed: 9012818]
33. Sala A B-MYB, a transcription factor implicated in regulating cell cycle, apoptosis and cancer. European journal of cancer 2005; 41: 2479–2484. [PubMed: 16198555]
34. Schmit F, Korenjak M, Mannefeld M, Schmitt K, Franke C, von Eyss B et al. LINC, a human complex that is related to pRB-containing complexes in invertebrates regulates the expression of G2/M genes. Cell cycle 2007; 6: 1903–1913. [PubMed: 17671431]
35. Schneider CA, Rasband WS, Eliceiri KW. NIH Image to ImageJ: 25 years of image analysis. Nature methods 2012; 9: 671–675. [PubMed: 22930834]
36. Solin LJ, Gray R, Baehner FL, Butler SM, Hughes LL, Yoshizawa C et al. A multigene expression assay to predict local recurrence risk for ductal carcinoma in situ of the breast. Journal of the National Cancer Institute 2013; 105: 701–710. [PubMed: 23641039]
37. Sotiriou C, Neo SY, McShane LM, Korn EL, Long PM, Jazaeri A et al. Breast cancer classification and prognosis based on gene expression profiles from a population-based study. Proceedings of the National Academy of Sciences of the United States of America 2003; 100: 10393–10398. [PubMed: 12917485]
38. Stein GH. T98G: an anchorage-independent human tumor cell line that exhibits stationary phase G1 arrest in vitro. Journal of cellular physiology 1979; 99: 43–54. [PubMed: 222778]
39. Tanaka Y, Patestos NP, Maekawa T, Ishii S. B-myb is required for inner cell mass formation at an early stage of development. The Journal of biological chemistry 1999; 274: 28067–28070. [PubMed: 10497154]
40. TCGA Research Network. Integrated genomic analyses of ovarian carcinoma. Nature 2011; 474: 609–615. [PubMed: 21720365]
41. Thorner AR, Hoadley KA, Parker JS, Winkel S, Millikan RC, Perou CM. In vitro and in vivo analysis of B-Myb in basal-like breast cancer. Oncogene 2009; 28: 742–751. [PubMed: 19043454]

42. Tripathi S, Pohl MO, Zhou Y, Rodriguez-Frandsen A, Wang G, Stein DA et al. Meta- and Orthogonal Integration of Influenza "OMICs" Data Defines a Role for UBR4 in Virus Budding. Cell Host Microbe 2015; 18: 723–735. [PubMed: 26651948]

43. Ukleja M, Valpuesta JM, Dziembowski A, Cuellar J. Beyond the known functions of the CCR4-NOT complex in gene expression regulatory mechanisms: New structural insights to unravel CCR4-NOT mRNA processing machinery. BioEssays : news and reviews in molecular, cellular and developmental biology 2016; 38: 1048–1058.

44. Yen HC, Xu Q, Chou DM, Zhao Z, Elledge SJ. Global protein stability profiling in mammalian cells. Science 2008; 322: 918–923. [PubMed: 18988847]

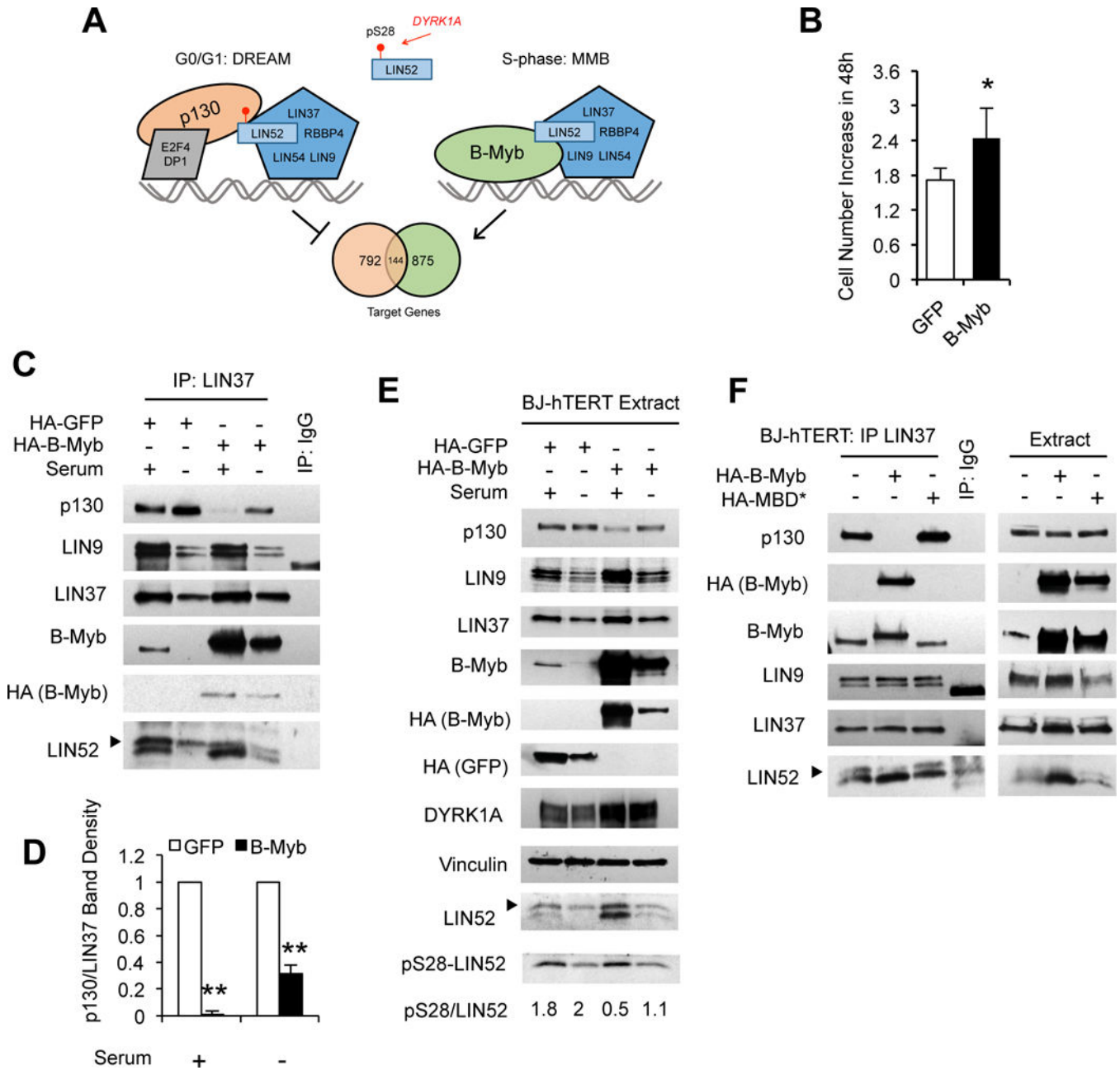

Figure 1. Effect of B-Myb overexpression in BJ-hTERT cells.

(A) Schema of the DREAM (repressor) and MMB (activator) complexes that use a common MuvB core (pentagons) to regulate both unique and shared target genes (Venn diagram) [6, 18, 29]. **(B)** Increased proliferation of BJ-hTERT cell line expressing HA-B-Myb compared to HA-GFP (control). Graph shows average increase (N=3) of cell density on day 5 relative to day 3 after plating, to account for differences in plating efficiency between the cell lines (* - $p<0.05$). **(C)** IP/WB analysis of DREAM and MMB complexes in BJ-hTERT fibroblasts stably expressing HA-GFP (control) or HA-B-Myb. Where indicated, cells were incubated without serum for 48h to promote DREAM complex formation. **(D)** Quantification of **1C**. Relative abundance of p130 to LIN37 in B-Myb overexpressing cells was compared to that

in the HA-GFP control cells (taken as 1). Graph shows average ± stdev of four independent experiments (** - $p<0.01$). **(E)** IP/WB analysis of BJ-hTERT cell lines stably expressing HA-tagged GFP control, WT B-Myb, or MuvB-binding deficient mutant (MBD) B-Myb. pS28/LIN52 ratio shows changes in pS28-LIN52 band density relative to the total LIN52 (both forms combined). Solid black arrow indicates pS28-LIN52 band here and throughout remaining figures. Vinculin blot is shown to confirm equal loading. **(F)** IP/WB analysis for DREAM/MMB assembly in BJ-hTERT cells stably expressing HA-GFP (control), HA-tagged WT or MuvB-binding deficient mutant (MBD) B-Myb.

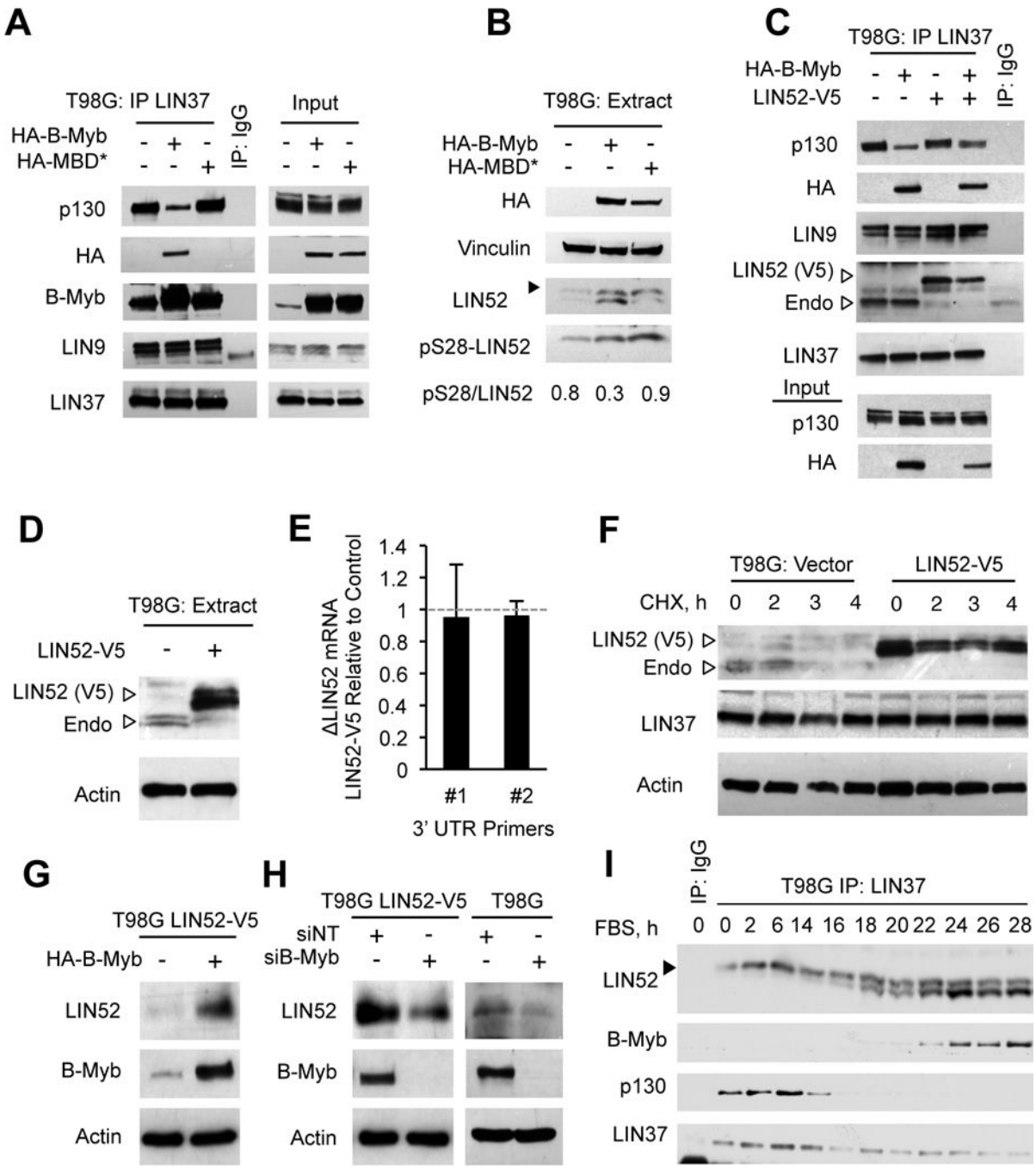

Figure 2. Effects of B-Myb and LIN52 overexpression in T98G cells reveal regulation at the protein level.

(A) IP/WB analysis of parental T98G cells compared with those stably expressing HA-tagged WT or MuvB-binding deficient mutant (MBD) B-Myb. **(B)** WB using extracts from the cells in **A** showing changes in LIN52 protein and relative abundance of pS28-LIN52. **(C)** IP/WB analysis of T98G cells stably expressing LIN52-V5, HA-B-Myb, or both, compared with control parental cells. Open arrow indicates position of the indicated proteins here and throughout the following figures. **(D)** WB analysis shows downregulation of endogenous

LIN52 in T98G cells stably expressing LIN52-V5. **(E)** RT-qPCR analysis with primers specific to endogenous LIN52 mRNA reveals no significant changes in the presence of ectopic LIN52. Graph shows average ± stdev (N=3, $p>0.05$). **(F)** WB analysis of cycloheximide (CHX) chase experiment using T98G stable cell lines expressing empty vector or LIN52-V5. **(G)** WB analysis of T98G cells stably expressing LIN52-V5 alone, or together with HA-B-Myb shows that B-Myb overexpression causes upregulation of the ectopically expressed LIN52. **(H)** Same as **G**, only after transient knockdown of B-Myb using siRNA. siNT, non-targeting siRNA control. **(I)** WB analysis of indicated proteins co-immunoprecipitated with LIN37 during cell cycle re-entry in T98G cells. Cells were synchronized in G0/G1 by serum starvation, released by adding 15% serum, and collected at different time points.

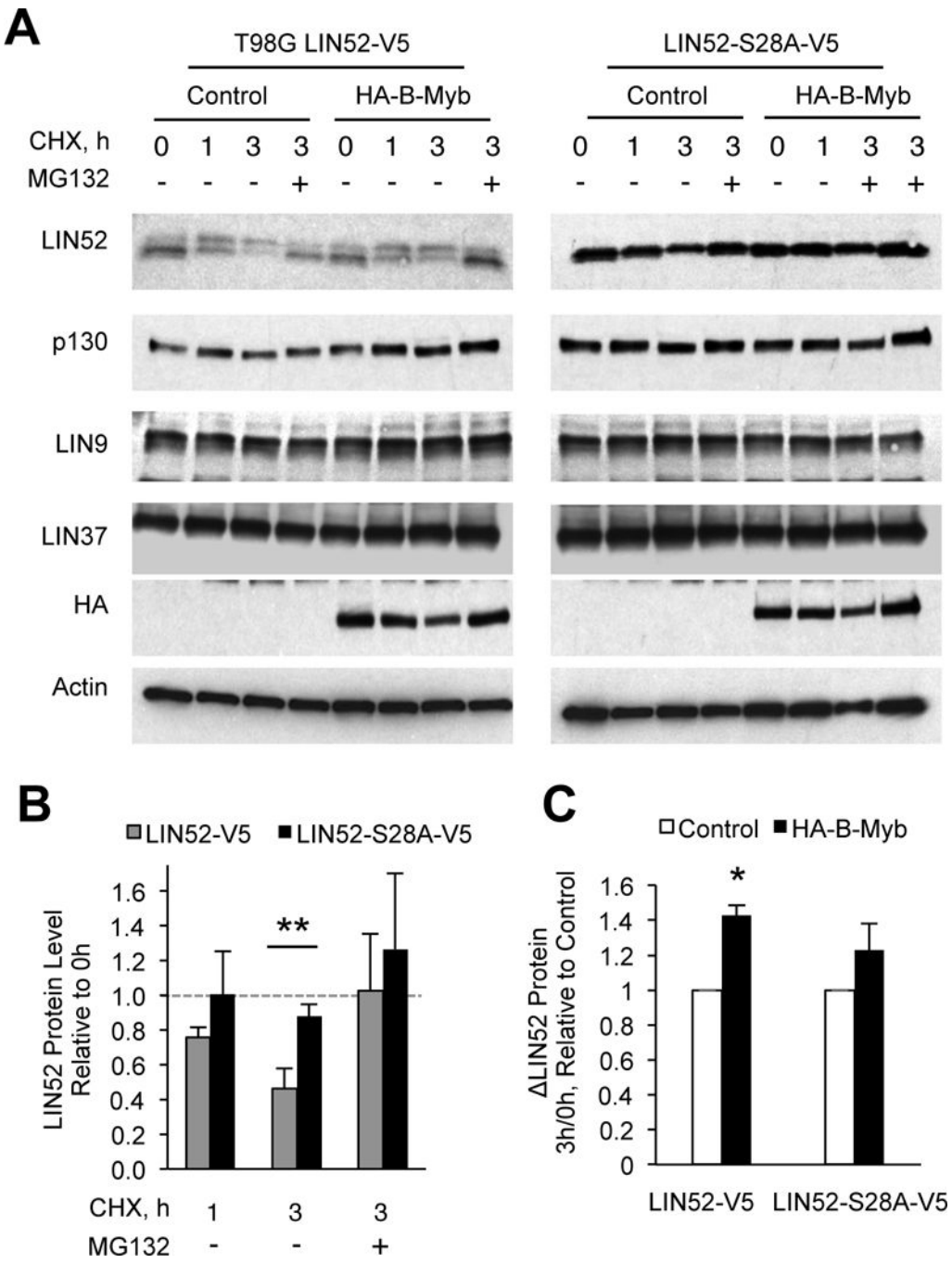

Figure 3. B-Myb overexpression in T98G cells stabilizes LIN52 but not S28A-LIN52 mutant.

(A) Representative immunoblots show CHX chase assays using T98G cells stably expressing LIN52-V5 or LIN52-S28A-V5 proteins alone, or together with HA-B-Myb. **(B, C)** Quantitative analysis of LIN52-V5 and LIN52-S28A-V5 CHX chase assays shown in **3A**. In panel **B,** graph represents average ± stdev (N=5) of LIN52 LIN52-S28A band density in control cells without B-Myb overexpression. LIN52 band density was first normalized to actin and then plotted relative to 0h (** - $p<0.01$). In panel **C,** graph shows the average change in LIN52 band density at 3h compared to 0h, in the presence of HA-B-Myb relative

to that in the control cells. Note that LIN52-V5 stability in the presence of HA-B-Myb is significantly greater than in cells expressing LIN52-V5 alone (N=3, * - $p<0.05$) whereas LIN52-S28A-V5 is not significantly affected by HA-B-Myb.

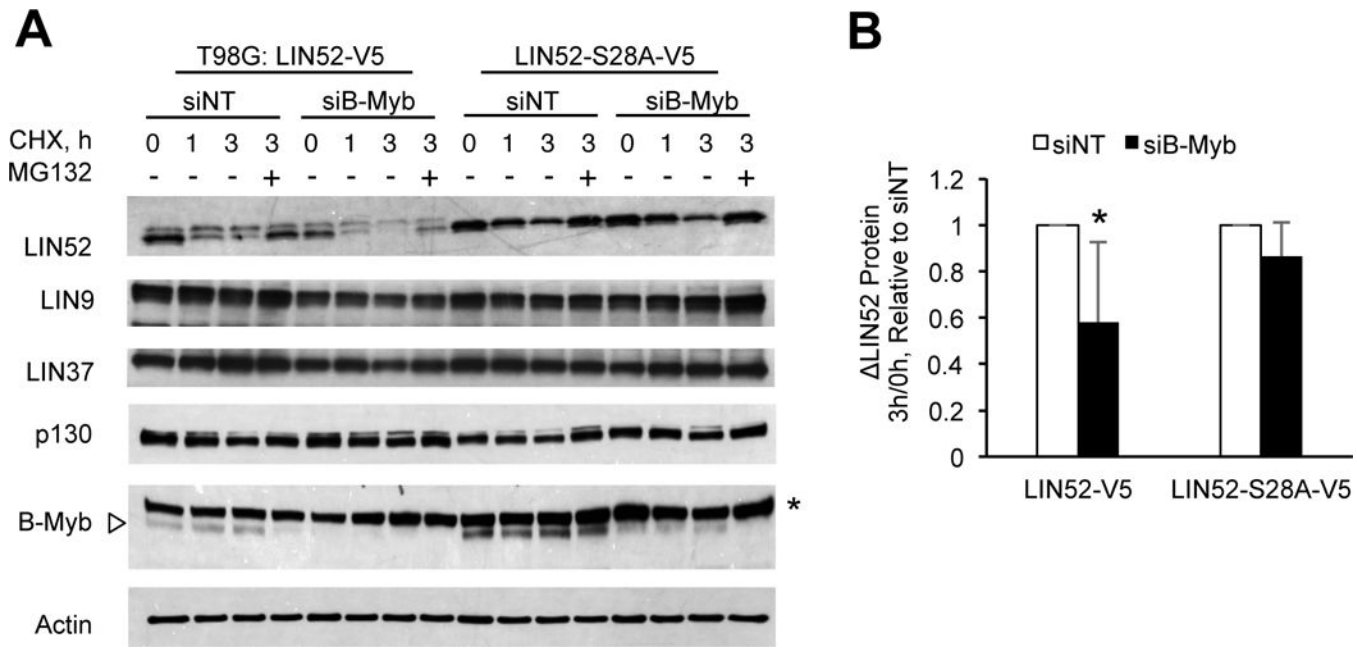

Figure 4. Depletion of B-Myb in T98G cells increases turnover of LIN52 but not the S28A-LIN52 mutant.

(A) Representative immunoblots show that RNAi knockdown of B-Myb decreases stability of wild type LIN52, but not LIN52-S28A-V5. T98G cells stably expressing LIN52 proteins were transfected with siNT (non-targeting) or B-Myb-specific siRNA, and used for CHX chase assays after 36 hours. Note the relative stability of LIN9 and LIN37 compared with that of LIN52. Asterisk indicates non-specific band. **(B)** Graph shows average change in LIN52 band density at 3h compared to 0h, in siB-Myb transfected cells relative to that in siNT cells. Note that LIN52-V5 stability in the presence of siB-Myb is significantly lower than in siNT-transfected cells (N=3, * - $p<0.05$) whereas LIN52-S28A-V5 is not significantly affected.

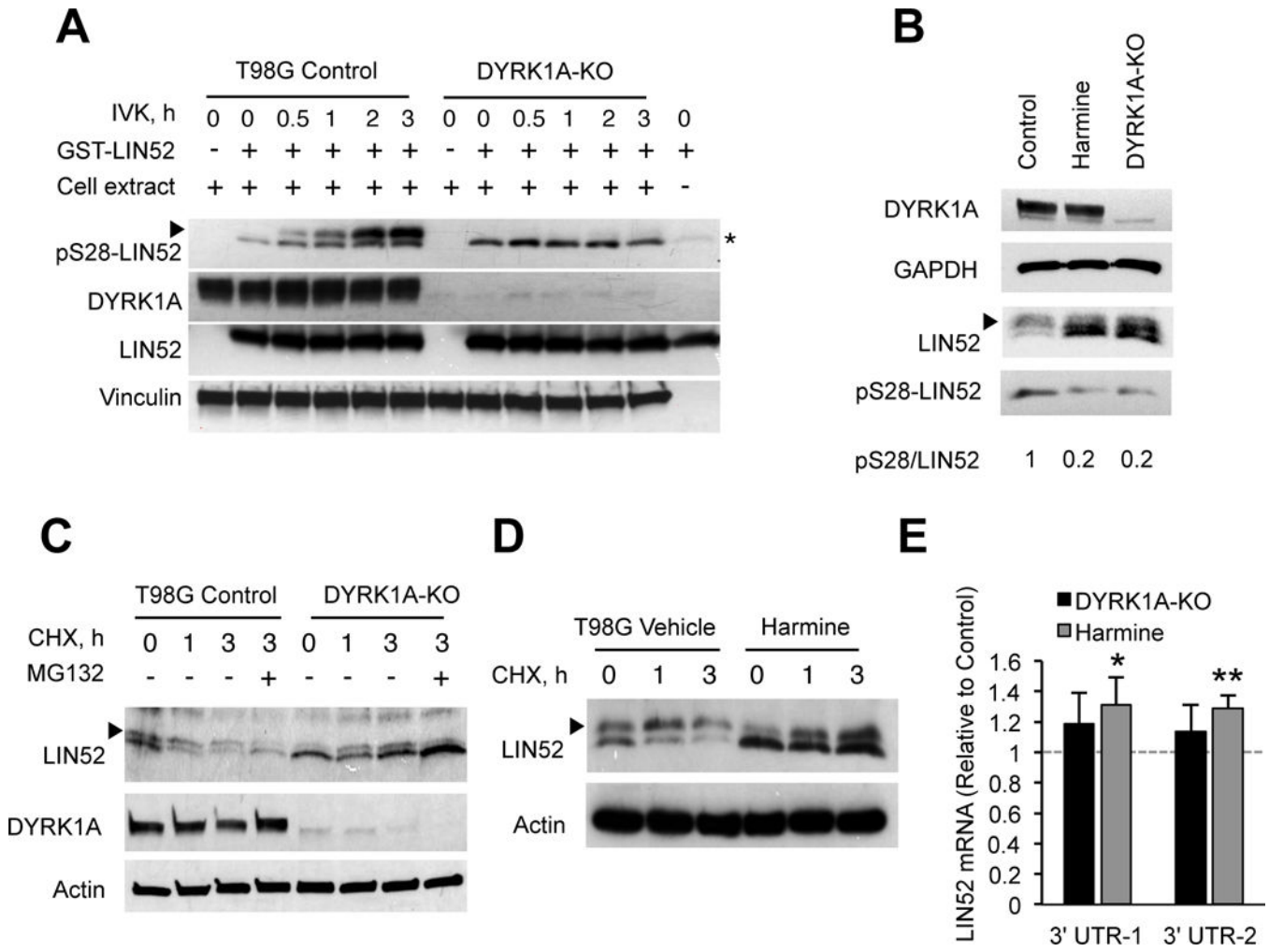

Figure 5. Phosphorylation of LIN52 by DYRK1A at S28 regulates its stability.

(A) *In vitro* kinase assay showing LIN52 phosphorylation at S28 by DYRK1A kinase in control T98G cells, but not in the DYRK1A-KO cells. GST-LIN52 was incubated with cell extracts in the presence of ATP as indicated. Presence of LIN52 phosphorylation at S28 as well as the total GST-LIN52 and DYRK1A, was assessed by WB. Asterisk denotes non-specific band. **(B)** WB analysis of the endogenous LIN52 and pS28-LIN52 in control T98G cells, DYRK1A knockout (KO) cells, or cells after harmine inhibition of DYRK1A kinase activity. **(C, D)** CHX chase assays show that endogenous LIN52 protein is more stable in DYRK1A-KO cells or in harmine-treated cells, as compared to control. **(E)** RT-qPCR analysis reveals a modest increase in LIN52 mRNA expression when DYRK1A is inhibited, as compared to control cells. Graph shows average ± stdev (N=3, * and ** correspond to p-value <0.05 and <0.01, respectively).

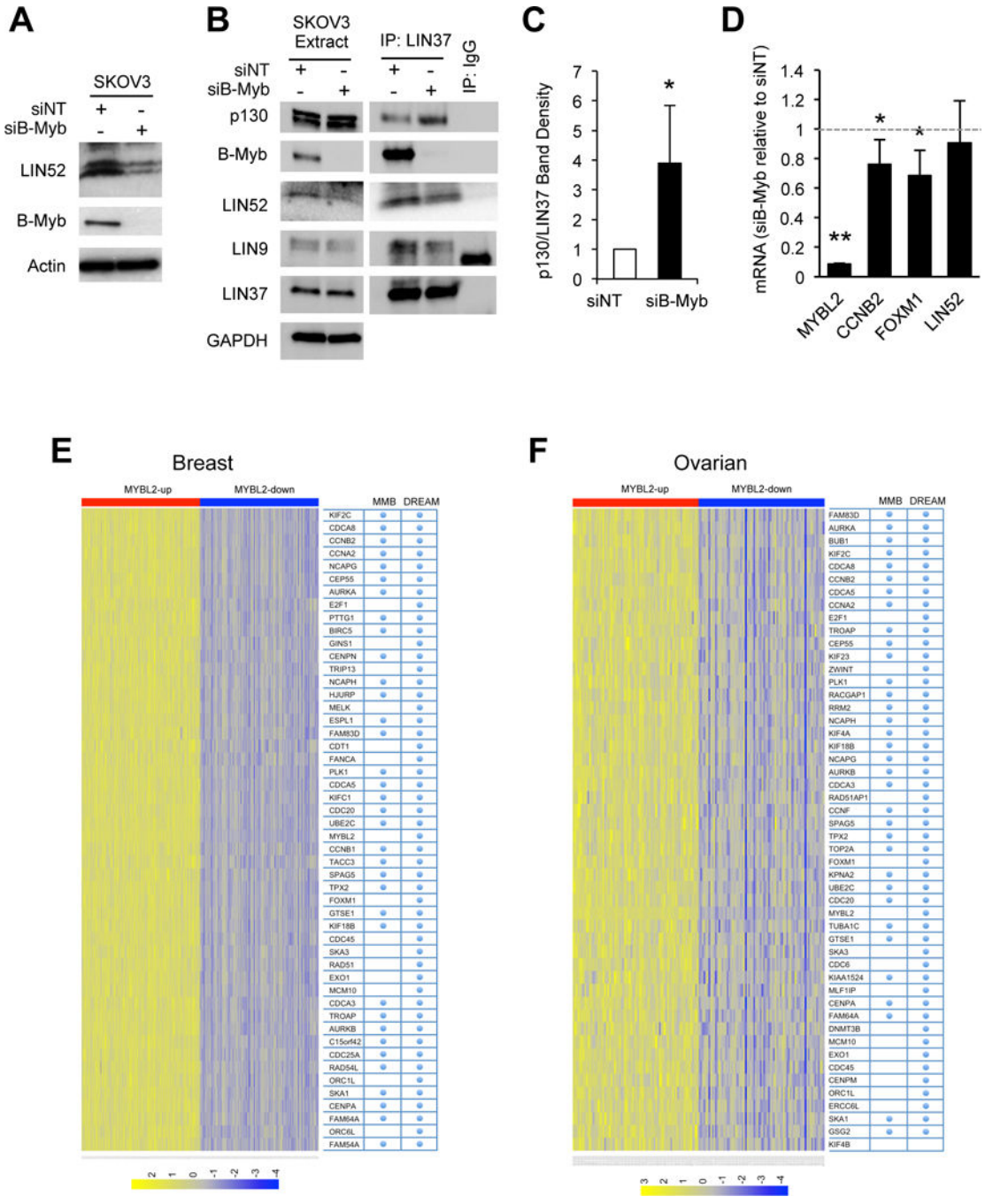

Figure 6. Effect of B-Myb on the DREAM complex function in cancer cells.

(A) WB analysis of the extracts from siRNA-transfected SKOV3 cells shows decreased expression of LIN52 in B-Myb-depleted cells compared to control. **(B)** IP/WB analysis shows increased binding of p130 to LIN37 (indicative of DREAM formation) in SKOV3 cells transfected with B-Myb-specific siRNA compared to control cells. **(D)** Quantification of **6B**. Relative abundance of p130 to LIN37 in siB-Myb transfected cells was compared to that in the siNT treated control cells (taken as 1). Graph shows average ± stdev of three independent experiments (* - $p<0.05$). **(D)** RT-qPCR analysis shows decreased expression of

FOXM1 (DREAM target) and *CCNB2* (DREAM and MMB target) genes upon B-Myb knockdown in SKOV3 cells. Graph shows average ± stdev of three independent experiments (* - $p<0.05$). **(E, F)** DREAM and MMB target genes are significantly upregulated in breast and ovarian cancers with high B-Myb expression (Fisher's exact test p-values 1.2^{-102} and 0.0065, respectively). Top 50 up-regulated genes in TCGA gene expression dataset of breast and ovarian cancer tumors with high expression of B-Myb are shown (χ^2 with Yates correction $p<0.001$). Genes were annotated as DREAM or MMB targets using http://www.targetgenereg.org [6].

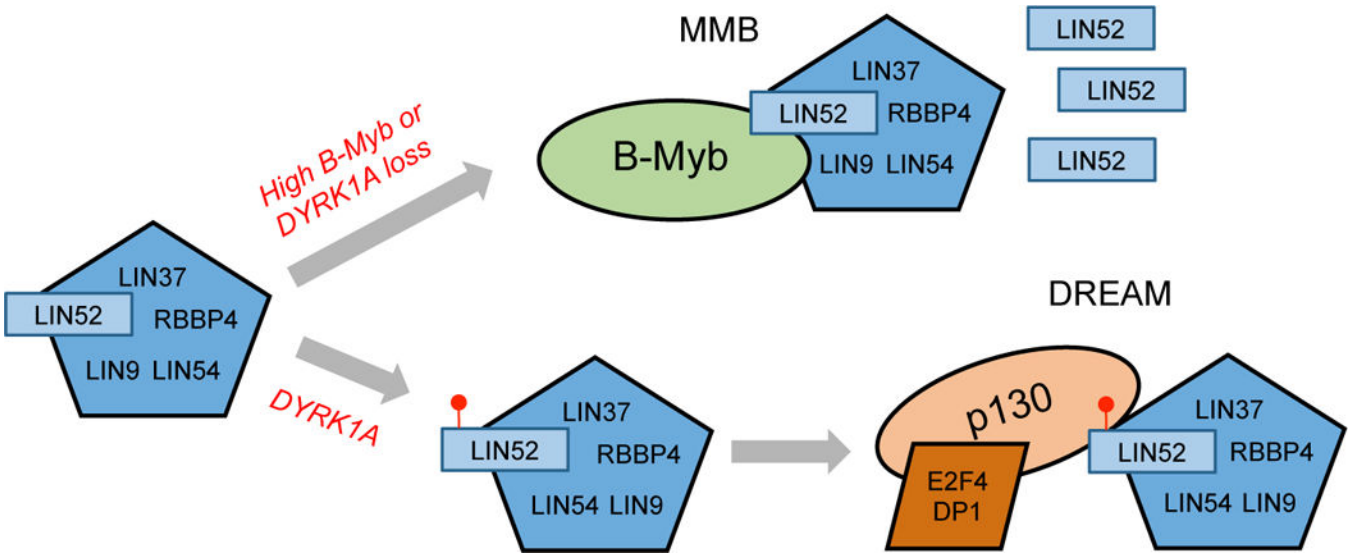

Figure 7: Model of opposing regulation of DREAM by B-Myb and DYRK1A.

High expression of B-Myb or inhibition of DYRK1A can interfere with DREAM assembly by promoting accumulation of un-phosphorylated LIN52, resulting in deregulation of cell cycle expression in cancer.